Chin. J. Astron. Astrophys. Vol. 3 (2003), No. 3, 247–256
(http://www.chjaa.org or http://chjaa.bao.ac.cn)

Chinese Journal of Astronomy and Astrophysics

A Fluid Dynamics Approach for the Computation of Nonlinear Force-Free Magnetic Field *

Jing-Qun Li [1,2], Jing-Xiu Wang [1] and Feng-Si Wei [2]

[1] National Astronomical Observatories, Chinese Academy of Sciences, Beijing 100012; lee@ourstar.bao.ac.cn

[2] Center for Space Science and Applied Researches, Chinese Academy of Sciences, Beijing 100080

Received 2002 November 14; accepted 2003 April 22

Abstract Inspired by the analogy between the magnetic field and velocity field of incompressible fluid flow, we propose a fluid dynamics approach for computing nonlinear force-free magnetic fields. This method has the advantage that the divergence-free condition is automatically satisfied, which is a sticky issue for many other algorithms, and we can take advantage of modern high resolution algorithms to process the force-free magnetic field. Several tests have been made based on the well-known analytic solution proposed by Low & Lou. The numerical results are in satisfactory agreement with the analytic ones. It is suggested that the newly proposed method is promising in extrapolating the active region or the whole sun magnetic fields in the solar atmosphere based on the observed vector magnetic field on the photosphere.

Key words: Sun: magnetic fields — MHD — mathods: numberical

1 INTRODUCTION

It is essential to have a basic understanding of the large-scale dynamics of the magnetized plasma and magnetic fields of the Sun (Parker 2001). However, so far, there has been no direct measurement of magnetic fields in the solar corona where the primary magnetic energy release takes place in solar activities. As is well known, force-free magnetic field is believed to be a good approximation to the coronal magnetic field, it is described by the following equations

$$\boldsymbol{B} \times (\nabla \times \boldsymbol{B}) = \boldsymbol{0}, \tag{1}$$

$$\nabla \cdot \boldsymbol{B} = 0\,. \tag{2}$$

Reconstruction of the magnetic structures in the solar atmosphere based on the force-free field assumption is of importance both in observational studies of magnetic activity, e.g., coronal mass ejection (Zhang, Wang & Nitta 2001), and in theoretical and numerical approaches (Ji &

* Supported by the National Natural Science Foundation of China.

Song 2001; Chen, Fang & Ding 2001). A variety of methods have been proposed to solve the force-free magnetic field equations. These methods are broadly classified into three classes by McClymont et al. (1997), namely, the extrapolation methods, current-field iteration methods and quasi-physical evolutionary methods. See references (McClymont et al. 1997; Wang 1999) for rather comprehensive reviews on this classification and some commonly used methods.

In addition to the methods cited in the above references, Wheatland et al. (2000) presented an optimized approach for reconstructing force-free magnetic fields. Their method is based on minimizing the global departure of an initial field from a free-force and solenoidal state. Also, an evolutionary procedure is used. Amari et al. (1997) discussed the mathematics encountered in attempts to reconstruct the force-free coronal magnetic field from the observed photospheric magnetic values. They also presented a potential vector Grad-Rubin-like method and a 3-D MHD evolutionary method.

The methods mentioned above are faced with a common issue: the results are difficult to satisfy the divergence-free condition. In this paper, we propose a new computational approach. One of the advantages of the newly proposed method is that the numerical solution is effectively forced to satisfy the divergence-free equation, by explicitly including the equation into the computation. The core of the method is as follows. Inspired by the analogy between the magnetic field and the velocity field of incompressible flow, we treat the magnetic field as an incompressible fluid velocity field. Then by Bernoulli's principle for steady flow and through an appropriate choice of the pressure of the fluid on the boundary, we can make the velocity field to satisfy the Eqs. (1) and (2), the force-free magnetic equations. Accordingly, with this transformation, we can take full advantage of modern high resolution algorithms of computational fluid dynamics to solve the force-free magnetic field problem. Considering the rapid development made in computational fluid dynamics, this is really an attractive feature.

We use the analytic solution proposed by Low & Lou (1990) to test the new approach, and find that the computational result is in satisfactory agreement with the theoretical solution. Furthermore, considering that in the application of the method to the computation of the active region magnetic field, only the filed values on the photosphere are available, we propose a procedure to treat the upper and side boundary conditions. The method promises to be useful for computing the active region and full global nonlinear force-free coronal magnetic field.

2 COMPUTATIONAL PRINCIPLE

Consider the steady incompressible invisid fluid equations

$$\nabla \cdot \boldsymbol{v} = 0, \tag{3}$$

$$(\boldsymbol{v} \cdot \nabla)\boldsymbol{v} = -\frac{1}{\rho}\nabla p + \boldsymbol{f}. \tag{4}$$

Equation (4) can be cast into

$$\frac{1}{2}\nabla(\boldsymbol{v} \cdot \boldsymbol{v}) - \boldsymbol{v} \times (\nabla \times \boldsymbol{v}) = -\frac{1}{\rho}\nabla p + \boldsymbol{f}. \tag{5}$$

If $\boldsymbol{f}$ is potential force, then it can be denoted as

$$\boldsymbol{f} = -\nabla\phi\,. \tag{6}$$

By Bernoulli's principle, the equation

$$\frac{1}{2}|\boldsymbol{v}|^2 + \frac{p}{\rho} + \phi = \text{const.} \tag{7}$$

holds along any streamline. However, for two different streamlines the corresponding constants are generally different. If every streamline in the flow passes through the boundary of the volume occupied by the fluid, we can choose appropriate pressure on the boundary, such that the equation

$$\frac{1}{2}|\boldsymbol{v}|^2 + \frac{p}{\rho} + \phi = \text{const.} \tag{8}$$

holds on the boundary. Then by Bernoulli's principle, one has

$$\frac{1}{2}|\boldsymbol{v}|^2 + \frac{p}{\rho} + \phi = \text{const.} \tag{9}$$

for the whole fluid. Hence Equation(4) becomes

$$\boldsymbol{v} \times (\nabla \times \boldsymbol{v}) = \boldsymbol{0}. \tag{10}$$

In the above and later discussion the density ρ is taken to be unity.

In summary, the discussion has shown that, if every streamline in the incompressible invisid steady flow passes through the boundary of the volume occupied by the fluid, we can choose suitable pressure on the boundary, such that the following equations

$$\boldsymbol{v} \times (\nabla \times \boldsymbol{v}) = \boldsymbol{0}, \tag{11}$$

$$\nabla \cdot \boldsymbol{v} = 0 \tag{12}$$

are satisfied everywhere in the flow.

Since the coronal magnetic field is believed to be anchored on the photosphere surface, we can assume that every magnetic field line passes through the photosphere surface. Under this condition, if we have a velocity field which satisfies the invisid incompressible fluid equations

$$\nabla \cdot \boldsymbol{v} = 0, \tag{13}$$

$$(\boldsymbol{v} \cdot \nabla)\boldsymbol{v} = -\nabla p, \tag{14}$$

in the domain $r > R_\mathrm{s}$, and satisfies the following boundary conditions

$$\boldsymbol{v}(R_\mathrm{s}) = \boldsymbol{B}(R_\mathrm{s}), \tag{15}$$

$$p(R_\mathrm{s}) = \text{const.} - \frac{1}{2}|\boldsymbol{v}(R_\mathrm{s})|^2, \tag{16}$$

where R_s is the solar radius, $\boldsymbol{B}(R_\mathrm{s})$ is the observed photosphere magnetic field, then by the above discussion, the velocity result can be taken as the force-free magnetic field that agrees with the observed vector magnetic field on the photosphere.

3 COMPUTATIONAL SCHEME

A variety of computational methods have been developed in computational fluid dynamics to deal with the incompressible steady flow equations. Among them is the artificial compression method proposed by Chorin (1967), and improved by many other authors (Turkel 1987; Liu et al. 1998). In this method, time-dependent equations

$$\frac{\partial U}{\partial t} + \frac{\partial F(U)}{\partial x} + \frac{\partial G(U)}{\partial y} + \frac{\partial H(U)}{\partial z} = S, \tag{17}$$

where $U=(p,u,v,w)^T$, $F(U)=(\beta^2 u, p+u^2, vu, wu)^T$, $G(U)=(\beta^2 v, uv, p+v^2, wv)^T$, $H(U)=(\beta^2 w, wu, wv, p+w^2)^T$, $S=(0, \frac{1}{Re}\triangle u, \frac{1}{Re}\triangle v, \frac{1}{Re}\triangle w)$ in domain $r>R_{\rm s}$, and

$$\boldsymbol{v}(R_{\rm s}) \;=\; \boldsymbol{B}(R_{\rm s}), \tag{18}$$

$$p(R_{\rm s}) \;=\; \text{const.} - \frac{1}{2}|\boldsymbol{v}(R_{\rm s})|^2 \tag{19}$$

are solved. Equation (17) has no physical meaning until the time derivative of p reaches zero, β is chosen to guarantee the hyperbolic property of Eq. (17), as well to reach a fast convergence rate and computational stability. It has been shown by Fortin et al. that the solution to Eqs. (17)–(19) will converge to the solution of steady equations, if the initial velocity is divergence-free (see Lecture Notes in Physics, Vol. 8, pp.337–342, Springer-Verlag, New York, 1971). However, our computation shows convergence even for the initial velocity prescribed by Eq. (20). For a good presentation of Chorin's method, see page 144–159 of (Peyret & Taylor 1983) and its references. It also describes other methods for incompressible fluid flow. During the computation, the Reynolds number Re is variable and tends to infinity with time, so that the limit solution satisfies the invisid equations.

In our test computation, the domain is taken to be $\{(x,y,z)|-1{\le}x{\le}1, -1{\le}y{\le}1, 0{\le}z{\le}1\}$. The bottom physical boundary conditions are determined by Eqs. (15) and (16), and we assume the upper computational boundary condition is known or can be determined in some way (further described later in our test cases and the discussion part). The initial conditions within the computational domain are as follows:

$$\boldsymbol{v}_0(x,y,z) \;=\; 0, \tag{20}$$

$$p_0(x,y,z) \;=\; \text{const.} - \frac{1}{2}|\boldsymbol{v}_0(x,y,z)|^2. \tag{21}$$

On the boundary, the initial values are determined by the boundary conditions.

4 HIGH RESOLUTION RIEMANN SOLVER

In order to improve the accuracy of the result of computation, we take the MUSCL-Hancock algorithm (van Leer 1985), which is a high resolution algorithm based on a Riemann solver. The algorithm for the 1-D case is descried as follows:

Step1: Let

$$U_i(x) = U_i^n + \frac{x-x_i}{\triangle x}\triangle_i\ , \qquad x\in[x_{i-\frac{1}{2}}, x_{i+\frac{1}{2}}]\,, \tag{22}$$

then we have

$$U_i^L \;=\; U_i^n - \frac{1}{2}\triangle_i, \tag{23}$$

$$U_i^R \;=\; U_i^n + \frac{1}{2}\triangle_i, \tag{24}$$

where

$$\triangle_i = \frac{1}{2}(1-\omega)(U_i^n - U_{i-1}^n) + \frac{1}{2}(1+\omega)(U_{i+1}^n - U_i^n), \qquad \omega\in[-1,1]\ . \tag{25}$$

Step 2: Calculate

$$\overline{U}_i^L \;=\; U_i^L + \frac{1}{2}\frac{\triangle t}{\triangle x}[F(U_i^L) - F(U_i^R)], \tag{26}$$

$$\overline{U}_i^R \;=\; U_i^R + \frac{1}{2}\frac{\triangle t}{\triangle x}[F(U_i^L) - F(U_i^R)]. \tag{27}$$

Step 3: Let

$$U_L = \overline{U}_i^R, \tag{28}$$

$$U_R = \overline{U}_{i+1}^L, \tag{29}$$

then solve the Riemann problem

$$U_t + F(U)_x = 0, \tag{30}$$

$$U(x,0) = \begin{cases} U_L, & \text{if } x < 0, \\ U_R, & \text{if } x > 0. \end{cases} \tag{31}$$

We have

$$\boldsymbol{F}_{i+\frac{1}{2}} = \frac{1}{2}(F_L + F_R) - \frac{1}{2}\sum_{i=1}^{m} \tilde{\alpha}_i |\tilde{\lambda}_i| \tilde{K}^{(i)}, \tag{32}$$

where $\tilde{\alpha}_i$, $\tilde{\lambda}_i$, and $\tilde{K}^{(i)}$ are determined by

$$U_R - U_L = \sum_{k=1}^{m} \tilde{\alpha}_k \tilde{K}^{(k)}, \tag{33}$$

$$F_R - F_L = \sum_{k=1}^{m} \tilde{\alpha}_k \tilde{\lambda}_k \tilde{K}^{(k)} \ . \tag{34}$$

Step 4:

$$U_i^{n+1} = U_i^n + \frac{\Delta t}{\Delta x}[\boldsymbol{F}_{i-\frac{1}{2}} - \boldsymbol{F}_{i+\frac{1}{2}}] \tag{35}$$

In the 3-D case, we make use of the finite volume method. The above steps can be applied to determine the flux across every surface of the cells.

5 TEST CASES

The procedures itemized above are tested by using the nonlinear force-free analytic solutions proposed by Low & Lou (1990). In the first test, the analytic solution is taken to be

$$\boldsymbol{B} = \frac{1}{r\sin\theta}\Big(\frac{1}{r}\frac{\partial A}{\partial \theta}\hat{r} - \frac{\partial A}{\partial r}\hat{\theta} + Q\hat{\phi}\Big), \tag{36}$$

where $A = \frac{P(\cos\theta)}{r^n}$, $Q(A) = aA^{1+\frac{1}{n}}$ and $P(\mu)$ is determined by the equation

$$(1-\mu^2)\frac{\mathrm{d}^2 P}{\mathrm{d}\mu^2} + n(n+1)P + a^2\frac{1+n}{n}P^{1+2/n} = 0. \tag{37}$$

The parameters of the solution are as follows: $n = 1, m = 2, a^2 = 2.55, z_0 = -0.5, \Phi = 0$. The meaning of these parameters is as the same as in (Low & Lou 1990). This test consists of two phases. First, the theoretical analytic solution is taken as the initial condition and the boundary condition. Theoretically, the solution should remain at the original values. However, it does evolve due to numerical error of discretization: the numerical divergence of the theoretical solution is not zero, the maximum of the divergence reaches up to 140. After a period of evolution, the solution approaches a stable state, and the solution basically keeps constant after 100 seconds of evolution, the maximum of divergence is below 0.01. This solution is taken

as the "numerical" analytic solution, and will play a role in the checking of the precision of the second phase of the numerical test. See Fig. 2 (left) for the result.

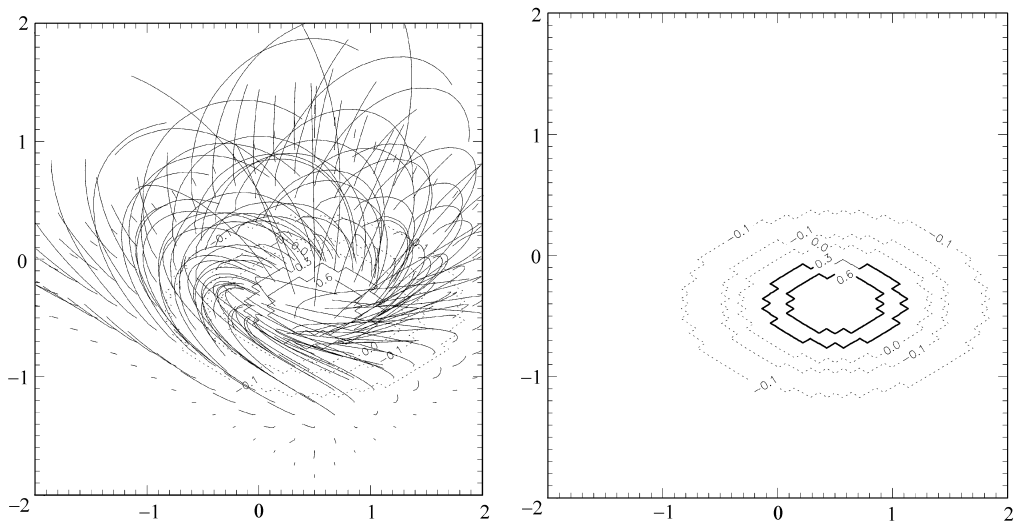

Fig. 1 Left: Theoretical analytic solution; Right: Contour of the Bz of the analytic solution.

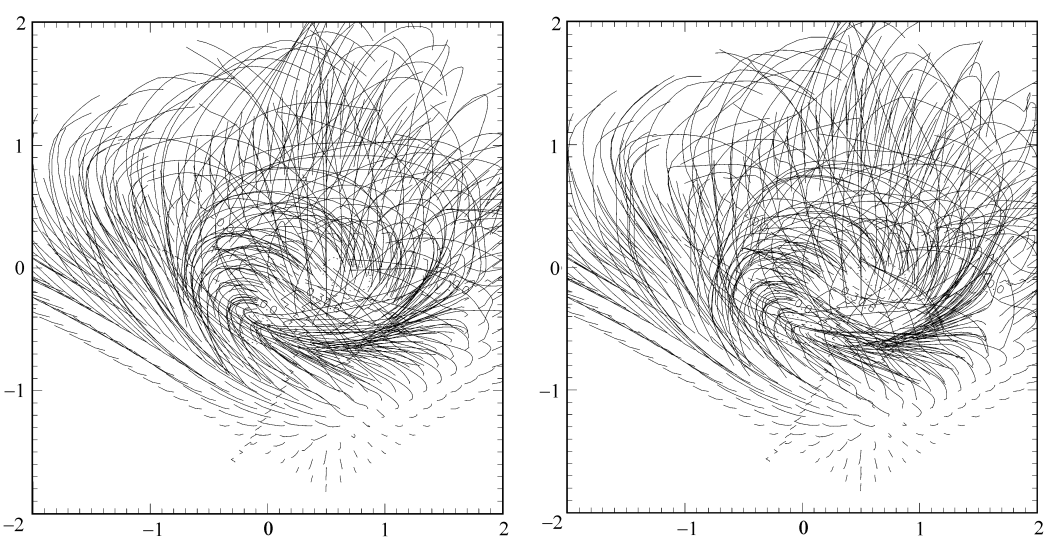

Fig. 2 Left: "Numerical" analytic solution; Right: Numerical solution.

In the second phase of the test, we take the boundary value of the analytic solution as our boundary condition, the initial values are obtained through linear interpolation of the upper and lower boundary values. After 200 seconds, the numerical solution reaches stable state, its

maximal divergence is below 0.01 again (Fig. 2, right). The difference between this solution and the one obtained in the first phase are also below 1%.

In the second test, the parameters are taken to be as follows: $n = 1, m = 2, a^2 = 2.55, z_0 = -0.5, \Phi = \frac{\pi}{2}$. The axis of symmetry of the above analytic solution is rotated to be parallel to the x-axis, so that in the computation domain, the solution is no longer axis-symmetric. The corresponding analytic and numerical results are shown in Figs. 3 and 4. Again, the numerical result is in good agreement with the analytic solution.

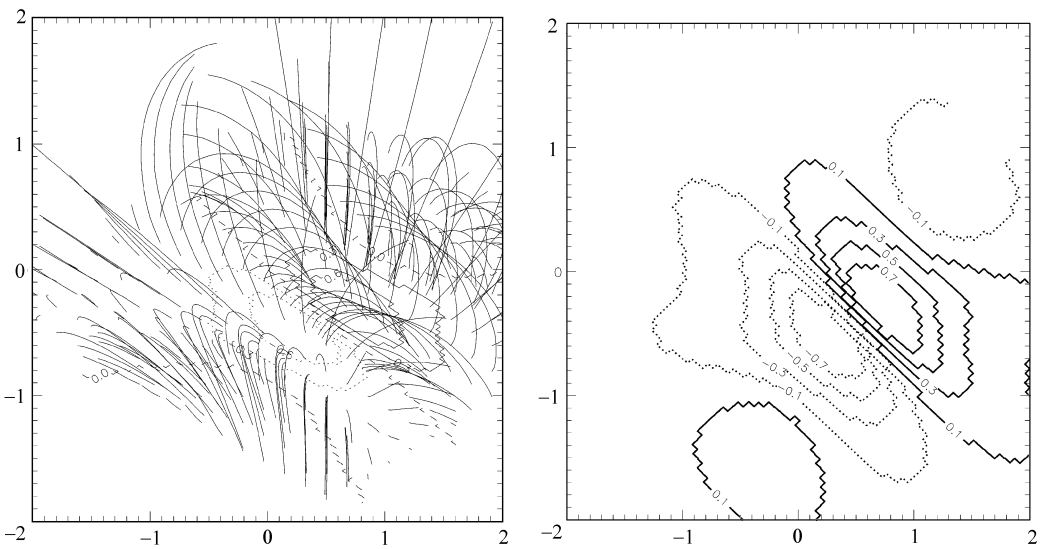

Fig. 3 Left: Theoretical analytic solution 2; Right: the Bz contours of the analytic solution 2.

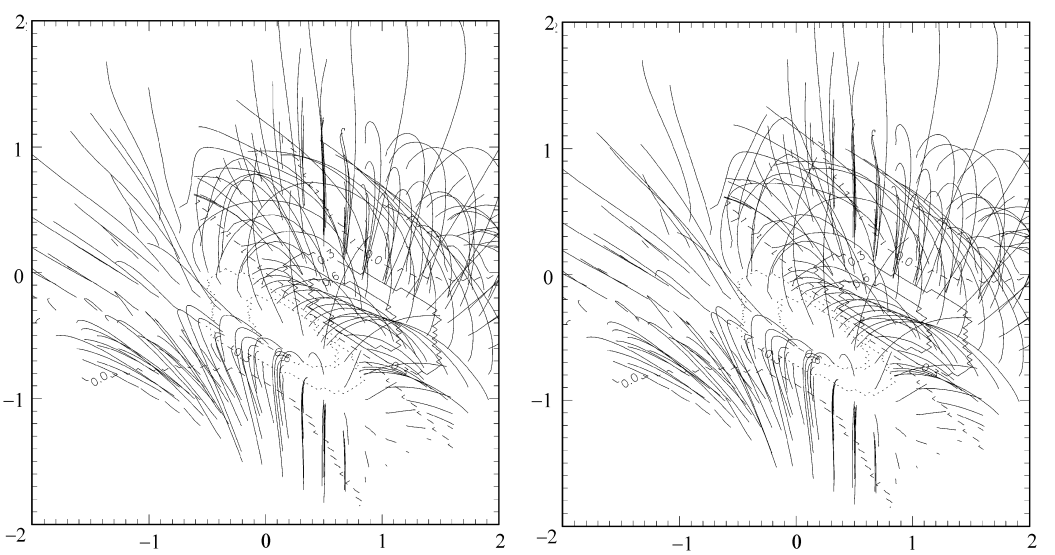

Fig. 4 Left: "Numerical" analytic solution 2; Right: Numerical solution 2.

Considering the situation in the practical application to the computation of the coronal magnetic field, we propose the following treatment on the side and upper boundary conditions.

Step 1, let

$$\nabla\phi = \boldsymbol{B}, \tag{38}$$

we are going to to solve the potential field problem:

$$\Delta\phi = 0, \tag{39}$$

$$\frac{\partial\phi}{\partial n}|_{z=0} = Bz(x, y, 0), \tag{40}$$

$$\phi(M) = O\Big(\frac{1}{r_{\rm OM}}\Big), \qquad \frac{\partial\phi}{\partial n} = O\Big(\frac{1}{r_{\rm OM}^2}\Big), \qquad (r_{\rm OM} \to \infty), \tag{41}$$

where $r_{\rm OM}$ denotes the distance between the origin and the point M. The solution to the above equation is

$$\phi(x_0, y_0, z_0) = \frac{z_0}{2\pi}\int_{-\infty}^{+\infty}\int_{-\infty}^{+\infty}\frac{\phi(x, y, 0)}{[(x - x_0)^2 + (y - y_0)^2 + z_0^2]^{\frac{3}{2}}}{\rm d}x{\rm d}y, \tag{42}$$

where

$$\phi(x, y, 0) = -\frac{1}{2\pi}\int_{-\infty}^{+\infty}\int_{-\infty}^{+\infty}\frac{Bz(x, y, 0)}{[(x - s)^2 + (y - t)^2]^{\frac{1}{2}}}{\rm d}s{\rm d}t\ . \tag{43}$$

Step 2, take the value of the above potential field on the side and upper boundaries as new side and upper boundary conditions, the bottom boundary values are taken to be the observed magnetic field values, then solve the force-free field using the procedure presented in Sec. 2 to Sec. 4.

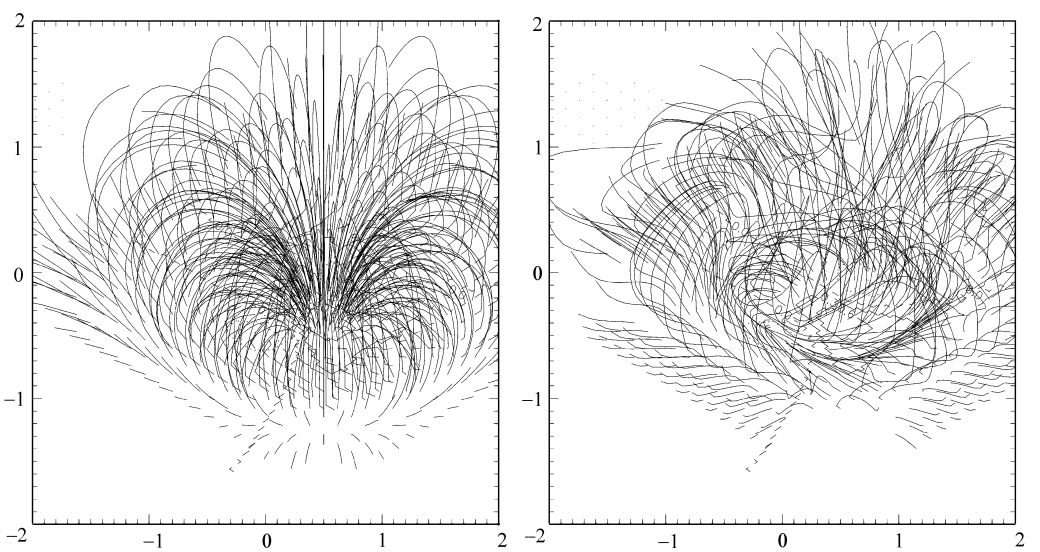

Fig. 5 Left: potential solution; Right:force-free solution.

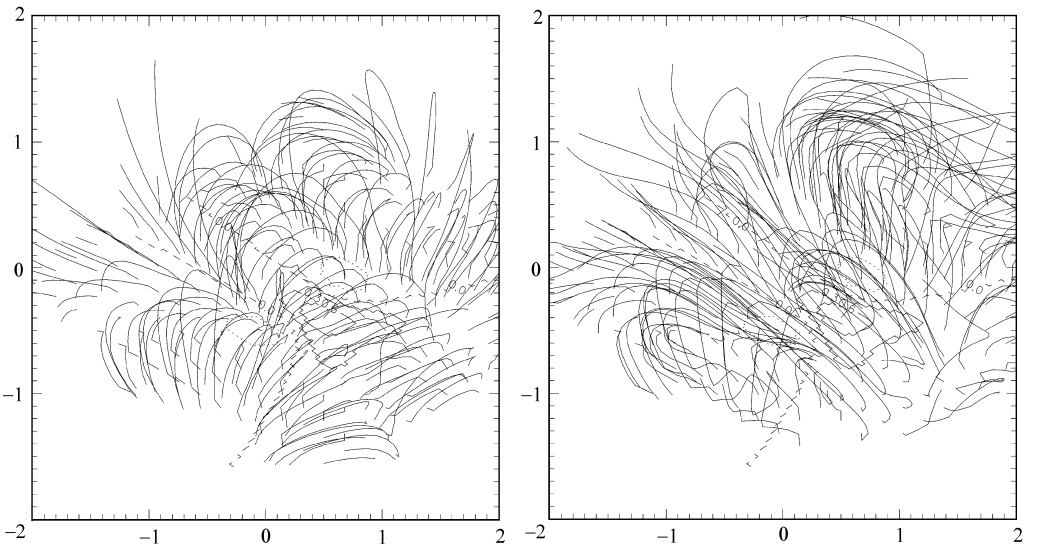

Fig. 6 Left: potential solution; Right: force-free solution.

Using this procedure, we also take the third and fourth test on our algorithm. The results are shown in Figs. 5 and 6, where the left panel shows the potential field solution, while the right panel shows the corresponding force-free solution. The related parameters in test 3 and test 4 are the same as in test 1 and test 2, respectively.

6 DISCUSSION

By the analogy between the fluid velocity fields in incompressible steady flows and magnetic fields, we have proposed a new fluid dynamics approach for computing force-free magnetic field. The new method has the advantage of automatically satisfying the divergence-free constraint. Moreover, the force-free coefficient α, which is generally unknown and sticky to treat, does not appear explicitly in our algorithm, as it does in many other methods. The artificial compression method is used to solve the steady flow equations, Eqs. (13) and (14), with the boundary values based on the analytic solution proposed by Low & Lou (1990), and the zero field as the initial condition.

In our test computation, the boundary values are taken to be fixed during the computation, in future improvement of the algorithm, the nonreflecting boundary conditions (Hu et al. 1984) or other methods will be taken to improve the numerical precision.

Considering the rapid development of the numerical methods made in the computational fluid dynamics, the new approach is promising and will evolve with new development of incompressible fluid dynamics computational methods .

Acknowledgements We are very grateful to Professor Y. Q. Hu for valuable discussion. We also thank the referee for his pertinent and constructive advice on the manuscript. The work is supported by National Key Basic Science Foundation (G2000078404), National Natural Science Foundation of China (19973009) and 40074044, 49990450.

References

Heiser A. M., Hardie R. H., 1964, ApJ, 140, 694
Aly J. J., 1989, Solar Physics, 120, 19
Amari T., Aly J. J., Luciani J. F., Boulmezaoud T. Z., Mikic Z., 1997, Sol. Phys., 174, 129
Chen P., Fang C., Ding M., 2001, Chin. J. Astron. Astrophys., 1, 176
Chorin A. J., 1967, J. Comput. Phys., 2, 12
Hu Y. Q., Wu S. T., 1984, J. Comput. Phys., 55, 33
Ji H., Song M. T., 2001, ApJ, 556, 1017
Klimchuk J. A., Sturrock P. A., 1992, 385, 344
van Leer B., 1985, SIAM J. Sci. Stat. Comput., 5, 1
Liu C., Zheng X., Sung C. H., 1998, J. Comput. Phys., 139, 35
Low B. C., Lou Y. Q., 1990, ApJ, 352, 343
McClymont A. N., Jiao L., Mikić, Z., 1997, Solar Phys., 174, 191
Mikić Z., McClymont A. N., 1994, In: K. S. Balasubramaniam, G. W. Simon., eds., ASP Conf. Ser. Vol. 68, Solar Active Region Evolution: Comparing Models with Observations, San Francisco: ASP, p.225
Parker E. N., 2001, Chin. J. Astron. Astrophys., 1, 99
Peyret R., Taylor T. D., 1993, Computational methods for fluid flow,Springer-Verlag, New York
Sakurai T., 1989, Spa. Sci. Rev., 51, 11
Turkel E., 1987, J. Comput. Phys., 72, 277
Wang J., 1999, Fund. Cos. Phys., 20, 251
Wheatland M. S., Sturrock P. A., Roumeliotis G., 2000, ApJ, 540, 1150
Zhang J., Wang J., Nitta N., 2001, Chin. J. Astron. Astrophys., 1, 85